Beyond the Protein Matrix

Martinoli, Christian; Dudek, Hanna M.; Orru, Roberto; Edmondson, Dale E.; Fraaije, Marco; Mattevi, Andrea

Published in:
ACS Catalysis

DOI:
10.1021/cs400837z

Publication date:
2013

Supporting Information

Beyond the Protein Matrix:

Probing Cofactor Variants in a Baeyer-Villiger Oxygenation Reaction.

Christian Martinoli[*], Hanna M. Dudek[°], Roberto Orru[*†], Dale E. Edmondson[§], Marco W. Fraaije[°], Andrea Mattevi[*].

*Department of Biology and Biotechnology, University of Pavia, Via Ferrata 9, 27100 Pavia, Italy;

°Molecular Enzymology Group, Groningen Biomolecular Sciences and Biotechnology Institute, University of Groningen, Nijenborgh 4, 9747 AG Groningen, The Netherlands;

§Departments of Biochemistry and Chemistry, Emory University, 1510 Clifton Road, Atlanta, GA 30322, USA.

Corresponding Author e-mail: andrea.mattevi@unipv.it, m.w.fraaije@rug.nl

MATERIALS AND METHODS

Chemicals and reagents - Chemicals were purchased from Sigma, Merck, and Bio-Rad and used without any further purification unless otherwise stated. *Corynebacterium ammoniagenes* FAD synthetase was a kind gift from Prof. M. Medina (Dept. of Biochemistry, University of Zaragoza, Spain).

Synthesis of FAD analogues – 8-Cl, 7,8-Cl, 7-Cl, and 8-nor, riboflavins were synthesized in the Edmondson laboratory as described.[1] 1-Deazariboflavin was a gift from Dr. D.B. McCormick, Emory Univ. They were converted to their respective FAD coenzyme forms using *Corynebacterium ammoniagenes* FAD synthetase.[2] In a typical experiment, a riboflavin derivative (100 µM) was incubated with 500 µM ATP, 10 mM $MgCl_2$, and 2 µM synthetase in 50 mM sodium phosphate buffer. The course of the reaction was monitored by thin-layer chromatography (cellulose plates in n-ButOH:HOAc:H_20

4:2:2, v/v/v) with detection using UV light. When conversion of the substrate was completed, FAD synthetase was removed by ultra-filtration. The flow-through was desalted on a C-18 Sep-Pack column (Waters®) and concentrated under reduced pressure. The samples were further purified by size-exclusion chromatography on columns packed with P2 gel (Biorad®) and eluted with distilled H_2O. Solvent was removed by lyophilization and the dry samples stored in the dark at -20° C until use.

Preparation of FAD analogue reconstituted enzymes - Wild type phenylacetone monooxygenase from *T. fusca* (PAMO) and the Arg337Lys mutant were expressed and purified as previously described (Fig. S1).[3] Pure protein solutions (15-20 μM)) were dialyzed in the dark for 20 hours against 2 L of deflavination buffer (4 M potassium bromide and activated charcoal in 100 mM potassium phosphate pH 6.5), which was changed several times. Subsequently, to remove the salt, extensive dialysis in 25 mM Tris/HCl pH 7.5 was performed or the sample was applied to a desalting column equilibrated with the same buffer. The resulting apo-protein was quantitatively recovered with its absorbance spectrum showing no flavin absorbance (Fig. S2). Its residual catalytic activity was < 1/200 of that of the holo-protein. The apo-protein was used for the reconstitution with FAD analogues by overnight incubation with 1.5 equivalents of the chosen analogue. For all analogues, the unbound cofactor was removed through cycles of dilution and concentration by ultra-filtration (Amicon® Ultracell®). High (>90%) values of incorporation were observed for FAD, 7-Cl,8-nor-FAD, 7,8-diCl-FAD, and 1-deaza-FAD whereas lower values were measured for 8-Cl-FAD (70%) and 5-deazaFAD (80%) (Fig. S2). The reconstituted holoproteins were stored at 4°C and remained stable for several days.

Steady-state kinetic measurements – Steady-state kinetics were performed at 25°C using a Varian Cary® 100 spectrophotometer in 25 mM Tris/HCl buffer pH 7.5. The solutions contained 100 μM NADPH (ε_{340}= 6.22 mM^{-1} cm^{-1}) or APADPH (ε_{363}= 9.1 mM^{-1} cm^{-1}), 0 – 1 mM phenylacetone, and 4.0 – 10 μM PAMO (evaluated from flavin absorbance). Kinetic parameters were determined by measuring

the decrease in absorbance of the NADPH, and the rates were measured in triplicate. NADPH and APADPH oxidase activities were determined in the same way, using NADPH or APADPH concentrations of 5 – 100 μM in the absence of the substrate. Uncoupling was probed using an oxygen electrode (Hansatech Oxygraph®). In these experiments, the production of H_2O_2 was monitored by the catalase assay.[4] Reactions were performed in a 1 ml vessel (2 μM PAMO, 500 μM of reducing cofactor, and 1 mM phenylacetone, if present) at 25°C and measured for 10 minutes, after which catalase was added. Values are averages of sixtuplicates.

Pre-steady-state kinetic measurements - Experiments were carried out using a stopped-flow apparatus equipped with a photodiode array detector (Applied Photophysics Ltd®). Enzyme solutions (15 μM in 25 mM Tris/Cl, pH 7.5) were made anaerobic by flushing them with nitrogen and removing oxygen traces by adding 10 mM glucose and catalytic amounts of glucose oxidase. The samples were reduced with anaerobic equimolar (slight excess) NADPH or APADPH dissolved in the same buffer containing 50 μM $NADP^+$. The rate of peroxyflavin formation (k_{ox}) and decay were then measured by mixing with oxygenated buffer (125 μM oxygen final concentration). All the experiments were performed at 25°C. Spectra were analyzed using Pro-K (Applied Photophysics Ltd®) by means of numerical integration methods, yielding the observed rate constants.

GC-MS assay - Substrate conversion reactions were carried out in 50 mM Tris/HCl pH 7.5 for 16 hours at 37 °C. The mixture contained 1.5 -3 μM PAMO, 100 μM APADPH or NADPH and 5 mM substrate (phenylacetone or thioanisole). As cofactor recycling system, phosphite dehydrogenase (7.5-15 μM) was used with 5 mM sodium phosphite. Each reaction was performed in duplicate. After overnight incubation, samples were analyzed for phosphate concentration using the molybdate assay and for the presence of the oxidation product using GC. Amount of phosphate corresponds to the amount of regenerated APADPH or NADPH:

PAMO: substrate + APADPH → product + $APADP^+$

phosphite dehydrogenase: $APADP^+$ + phosphite → APADPH + phosphate

Structural studies - Wild type and Arg337Lys proteins were crystallized by vapor diffusion at 4 °C using 1–3 µl of protein solutions (15 - 18 mg/ml in 0.5 µM FAD and 2 - 4 mM $APADP^+$, 50 mM Tris/HCl pH 7.5) mixed with equal volumes of reservoir containing 38% - 40% (w/v) PEG4000, 100 mM MES/HCl, pH 6.5, and 100 mM NaCl.[3] Crystallographic analyses were performed using programs of the CCP4 package.[5]

REFERENCES

1) Haley, E.E.; Lambooy, J.P. *J. Am. Chem. Soc.*, **1954**, *76*, 5093-5096.

2) Frago, S.; Martínez-Júlvez, M.; Serrano, A.; Medina, M. *BMC Microbiol.* **2008**, *8*, 160-168

3) Orru, R.; Dudek, H.M.; Martinoli, C.; Torres Pazmiño, D.E.; Royant, A.; Weik, M.; Fraaije, M.W.; Mattevi, A. *J Biol Chem.* 2011 286:29284-29291

4) Daithankar, V.N.; Wang, W.; Trujillo, J.R.; Thorpe, C. *Biochemistry* **2012**, *51*, 265-272

5) Winn, M.D.; Ballard, C. C.; Cowtan, K. D.; Dodson E.J.; Emsley, P.; Evans, P. R.; Keegan, R. M.; Krissinel, E.B.; Leslie, A. G.; McCoy, A.; McNicholas, S. J.; Murshudov, G. N.; Pannu, N. S.; Potterton, E. A.; Powell, H. R.; Read, R. J.; Vagin, A.; Wilson, K. S. *Acta Crystallogr D Biol Crystallogr*. **2011**, *67*, 235-242.

6) Vargo, D.; Pokora, A.; Wang, S. W.; Jorns, M. S. *J Biol Chem*. **1981**, *256*, 6027-6033.

7) Torres Pazmiño, D. E.; Baas, B. J.; Janssen D. B.; Fraaije, M. W., *Biochemistry* **2008**, *47*, 4082-4093

8) Schreuder, H. A.; Hol, W. G.; Drenth, J. *Biochemistry* **1990**, *29*, 3101-3108

SUPPLEMENTARY FIGURES AND TABLES

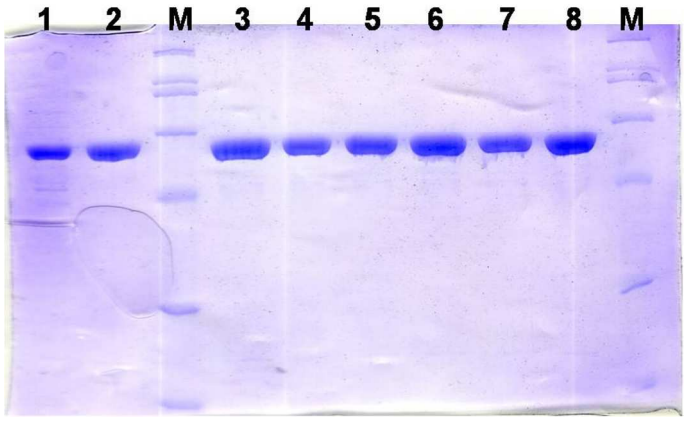

Figure S1. SDS-polyacrylamide gel shows no protein degradation during the procedures used for aproprotein generation and holoenzyme reconstitution: M molecular weight ladder; lanes 1-2, native PAMO at different stages of the purification protocol; lane 3, apo-PAMO; lane 4, 7-Cl,8-nor-PAMO; lane 5, 8-Cl-PAMO; lane 6, 7,8-diCl-PAMO; lane 7, 1-deaza-PAMO; lane 8, 5-deaza-PAMO.

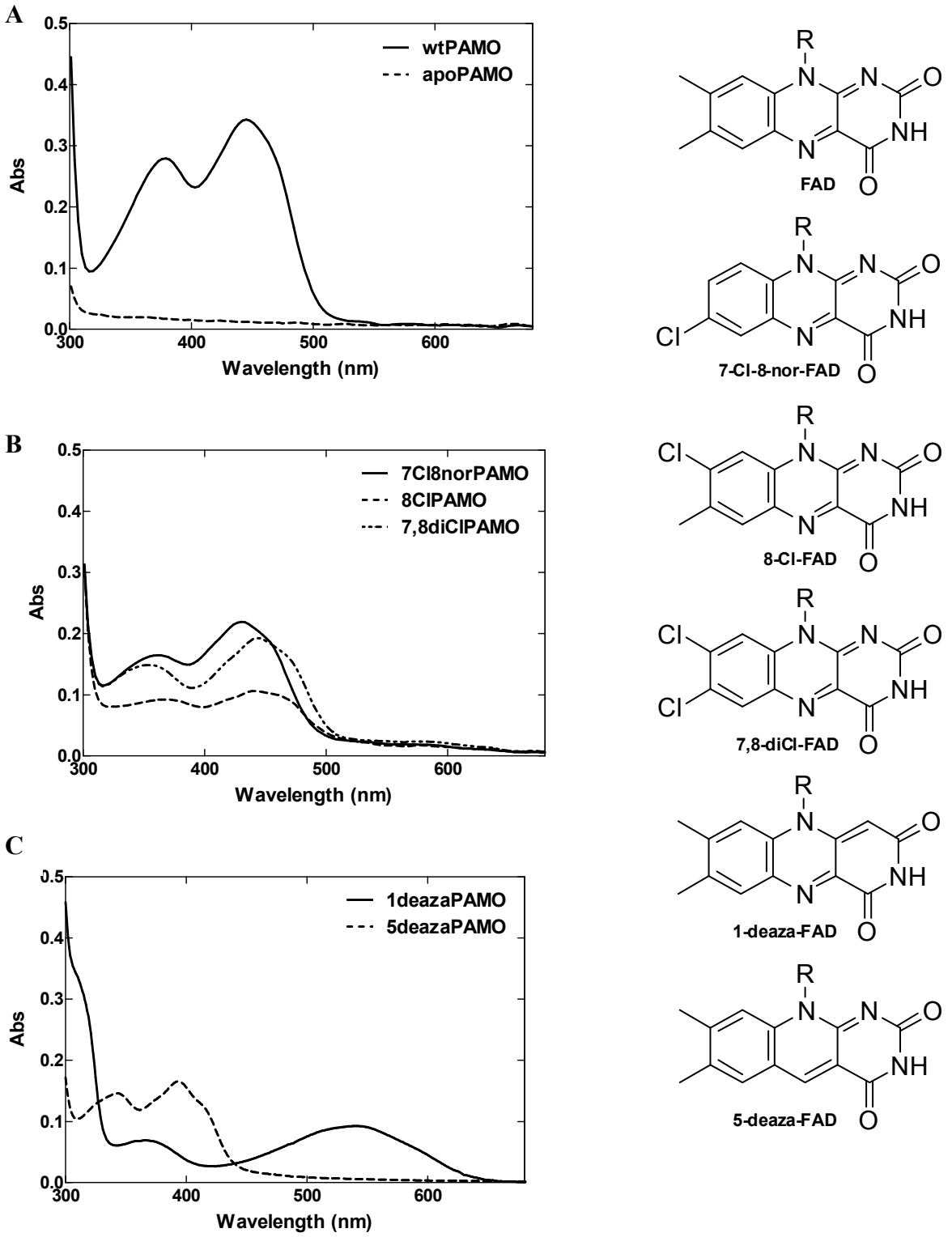

Figure S2. Absorbance spectra of: A) PAMO in holo and apo forms; B) the enzyme reconstituted with chloro-flavin derivatives, and C) PAMO bound to deaza-flavin derivatives. Protein concentrations are in 15-20 μM range. The right panel shows the structural formulas of the isoalloxazine moieties of the employed FAD derivatives.

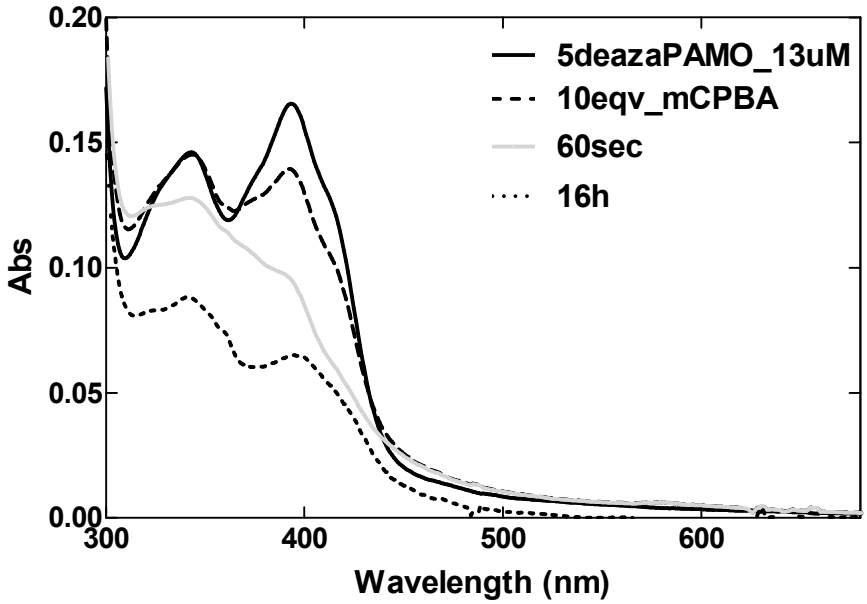

Figure S3. No NADPH-reduction of the protein-bound 5-deazaflavin (Fig. S2c) was detected, although incorporation of the flavin could be demonstrated by the typical reactivity with epoxidation agents. Indeed, the protein-bound modified cofactor reacts with m-chloroperoxybenzoate (mCPBA) to form an epoxide adduct as found for other reconstituted flavoproteins.[6] The reaction was performed with 13 μM enzyme in 50 mM sodium borate buffer at pH 9.3 mixing with 10 equivalents of reagent. The spectra were measured before mixing, immediately after mixing, after 1 minute, and after overnight incubation.

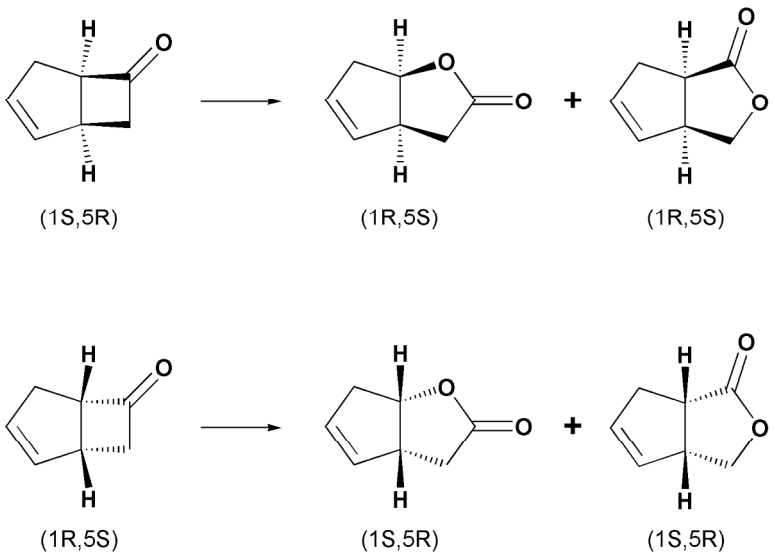

Figure S4. The Baeyer-Villiger oxidation of bicyclo[3.2.0]hept-2-en-6-one. Migration of the more substituted carbon atom generates the so-called "normal" lactone (left), while "abnormal" lactone is formed by migration of the less substituted carbon atom (right).

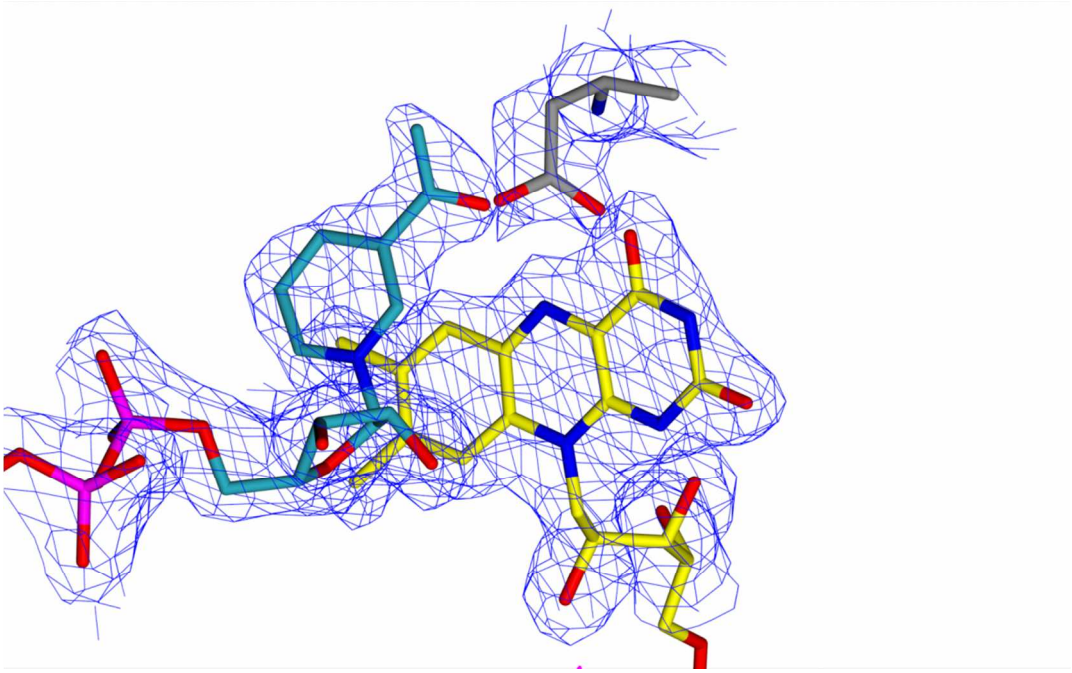

Figure S5. Final weighted 2Fo-Fc map for the structure of the reduced enzyme bound to $APADP^+$. The contour level is 1.4 σ. Protein carbons (Asp66) are in grey, flavin carbons in yellow, and $APADP^+$ carbons in light blue. The bound Cl^- ion is in dark red.

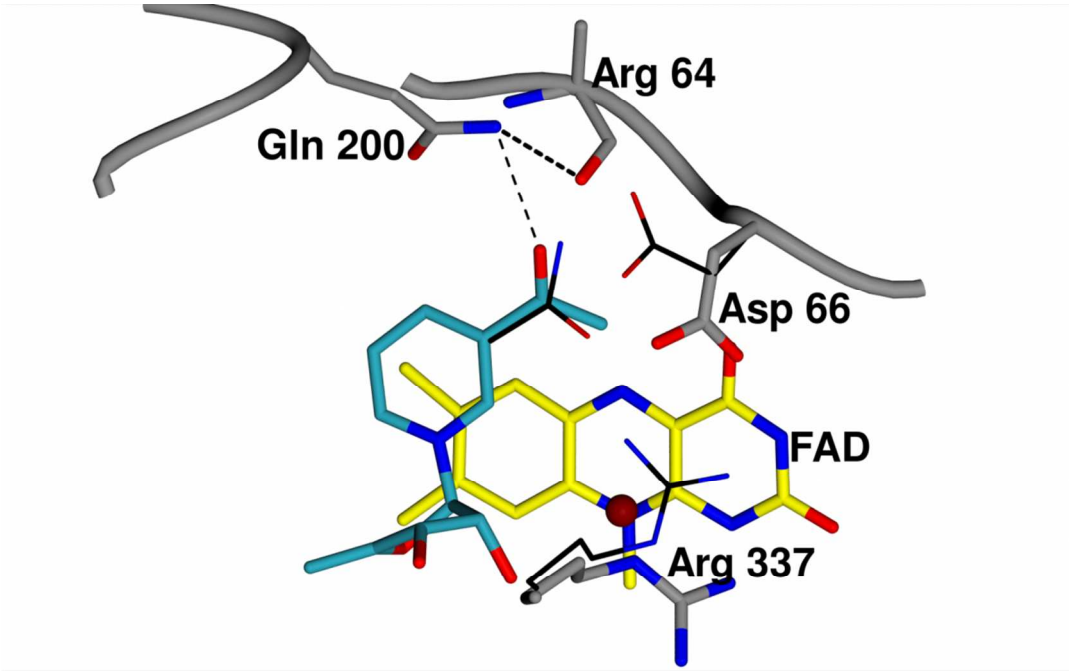

Figure S6. Active site conformation of oxidized PAMO bound to APADP+. Protein carbons are in grey, flavin carbons in yellow, and $APADP^+$ carbons in light blue. The bound Cl^- ion is shown as dark red sphere (a Cl^- atom in the same position is present also in the NADP+ complex). H-bonds are shown as dashed lines. The orientation of the acetyl group of bound $APADP^+$ was tentatively assigned based on the H-bonding environment. The side chains of Asp66 and Arg337 and the nicotinamide ring of the oxidized PAMO-$NADP^+$ complex (PDB entry 2YLR) are shown as thin lines with carbons in black. For the sake of clarity, the side chain of Arg64 is not shown.

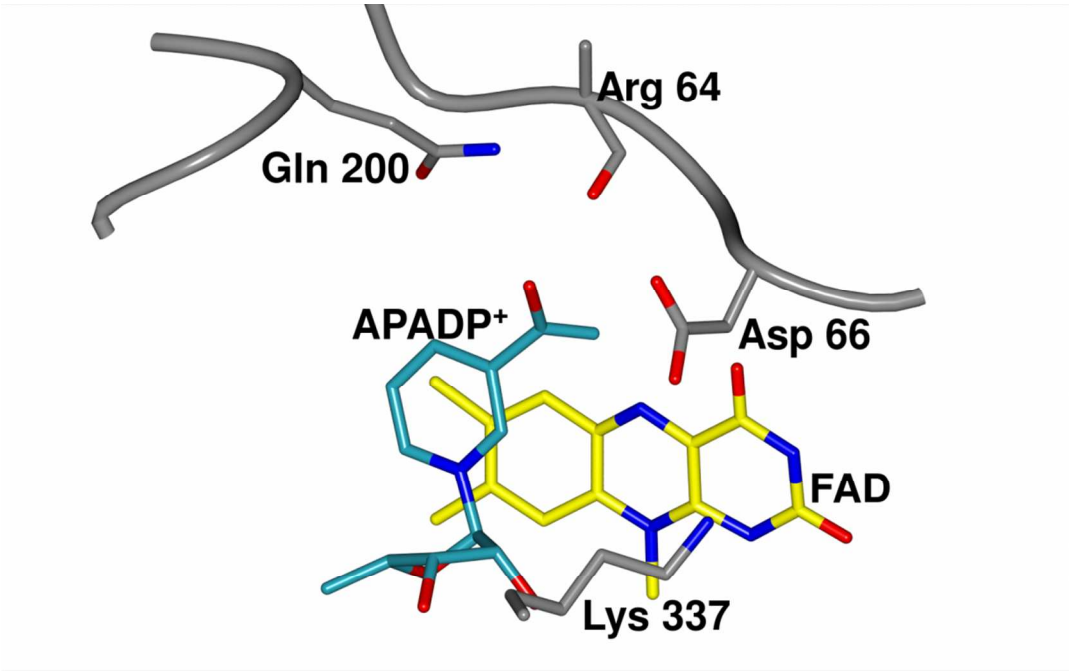

Figure S7. Active site conformation of oxidized Arg337Lys PAMO bound to $APADP^+$. Colors are as in Figure S6. Arg337Lys protein is unable to catalyze the oxygenation step but features a pronounced stabilization of the flavin-peroxide intermediate.[7] Remarkably, by contrast with the wild-type protein, the Arg337Lys protein retains such a strong intermediate stabilization also when APADPH is used as electron donor (Table 4). Consistently, the $APADP^+$-bound crystal structure of Arg337Lys does not exhibit the Asp66 rotation, which is in line with the notion that this conformational change crucially affects the oxygen-reaction of the $APADP^+$-bound wild-type PAMO (Fig. S7). The side chain of Arg64 is not shown.

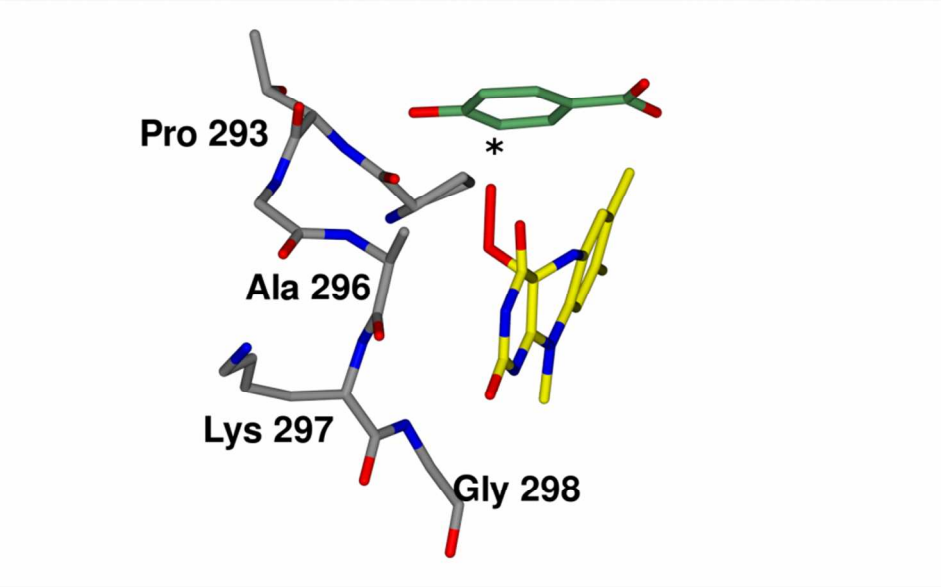

Figure S8. The flavin-peroxide intermediate modeled in the active site of product-bound *p*-hydroxybenzoate hydroxylase (PDB entry 1PBE). The asterisk outlines the site of hydroxylation on the substrate.[8]

Table S1. Coupling efficiency with APADPH

Enzyme (μM)	Phenylacetone			Thioanisole		
	PO_4^{3-} (mM)	benzylacetate (mM)	uncoupling (%)	PO_4^{3-} (mM)	thioanisole oxide (mM)	uncoupling (%)
1.5	2.3	0.7	70	4.2	1.6	62
3.0	4.4	1.3	70	5.3	3.0	44

Amount of phosphate corresponds to the amount of consumed APADPH. Reported values are average of two experiments. Very similar values of uncoupling were obtained using the oxygen electrode.

Table S2. Pre steady-state kinetic parameters

	NADPH		NADPH and phenylacetone		APADPH		APADPH and phenylacetone	
	k_{ox} (mM^{-1} s^{-1})[a]	Decay (s^{-1})	k_{ox} (mM^{-1} s^{-1})	Decay (s^{-1})	k_{ox} (mM^{-1} s^{-1})	Decay (s^{-1})	k_{ox} (mM^{-1} s^{-1})	Decay (s^{-1})
Wild-type	870[b]	0.01[b]	870[b]	73[b,c]	40	1.3	40	1.0
Arg337Lys	46[b]	0.001[b]	inactive		40	0.025	inactive	

[a] Errors are within ±15% of the measured values.

[b] From Torres Pazmiño et al. 2008.[7]

[c] A subsequent step of 4.1 s-1 occurs, probably due to conformational changes.[7]

Table S3. Crystallographic statistics

	Wild-type APADP$^+$ reduced	Wild-type APADP$^+$ oxidized	Arg337Lys – APADP$^+$ oxidized
PDB code	4C74	4OVI	4C77
Resolution[a] (Å)	2.0	1.9	2.70
Rmerge (%)	16.3 (99.5)	14.6 (82.3)	8.9 (45.4)
Completeness (%)	100 (100)	100 (100)	99.1 (99.6)
Unique reflections	47459	59226	19765
Redundancy	10.1 (10.4)	10.0 (9.8)	3.1 (3.2)
I/σ	7.7 (2.8)	9.1 (1.2)	8.2 (2.9)
$CC_{1/2}$ (%)	99.1 (87.3)	99.8 (46.4)	99.0 (81.4)
R_{cryst} (%)	23.5	22.2	19.3
R_{free} (%)	27.8	27.7	25.7
Rmsd bond lengths (Å)	0.02	0.02	0.01
Rmsd bond angles (°)	2.10	2.17	1.79

[a] The space group is $P3_221$ with unit cell axes $a=b=107.6$ Å and $c=106.5$ Å.